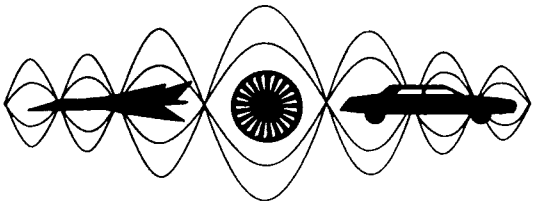

FIFTH INTERNATIONAL CONGRESS ON SOUND AND VIBRATION
DECEMBER 15-18, 1997
ADELAIDE, SOUTH AUSTRALIA

Resonant oscillations governed by the Boussinesq equation with damping

Sh.U.Galiev
Department of Mechanical Engineering, The University of Auckland, Private Bag
92019, Auckland 1, New Zealand

Abstract. It is shown that the perturbed Boussinesq type equations describe oscillations in different porous media (soils, rocks, bubbly liquids and so on). Nonlinear earthquake-induced vertical and horizontal waves in natural resonators (hills, basins and so on) are studied. Periodical resonant solutions of the above equations are constructed by the perturbation method. The solutions display on the one hand generation and interaction shock-, solitary- and cnoidal-type waves and on the other weak nonlinear interaction left-and right-hand side travelling waves. *Travelling oscillons* which can form *standing oscillons* are discussed. Nonlinear, off-resonant, dispersive, hysteresis, trap, topographical and dissipative effects which can take place in the natural resonators during earthquakes are defined. Theoretical results explain some anomalous data from the Northridge 1994 Southern California earthquake and also data of earthquake modelling.

1. Basic equations for the ground layer

Many of the world's cities are built on sedimentary basins or at the tops of ridges or near water basins. From the standpoint of earthquake risk, however, basins (valleys), hilltops and coastal regions are often the least desirable places to build. The topographies can form natural resonators , where seismic waves are amplified to shattering intensity. Theoretical calculations predict that crest amplifications with respect to the base can reach a factor of 30. The resonance of seismic waves in sedimentary basins was the reason for the collapse of about 300 buildings during the 1985 Mexico City earthquake [1]. A peak acceleration of 1.82g was recorded [2] during the Northridge 1994 Southern California earthquake. This record amplification of the ground motions at the Tarzana hill may be also explained by the resonance. Earthquake-induced oscillations of a bed (bottom) can generate a train of tsunami-like waves.

1.1. *Surface waves*

Recently there has been great interest in the physics of sand-like material lying on a vertically oscillating surface [3,4]. Different , very interesting wave phenomena were observed on the layer surface depending on the amplitude and frequency of excitation. These phenomena were usually connected with the parametric effect. However there are a possibility of a vertical excitation of the surface ground waves due to a topographical effect.

Following Airy's method [5, p. 259] we can write equations of motion and continuity for a viscoelastic (the Kelvin model) surface layer

$$\rho\, h u_{tt} = \sigma_x (h+\eta) \quad , \qquad h = (h+\eta)(1+u_x) \quad , \tag{1.1}$$

where t is time, x is a horizontal Lagrangian coordinate, u is a horizontal displacement, ρ is

the density, h is a variable thickness of a surface layer of the ground ($h= h(x)$), σ is a stress, η denotes an elevation of the surface, P is a hydrostatic pressure, and subscripts t and x, respectively, indicate the time and space derivatives. Let us assume that the some contribution to σ comes from the hydrostatic law which is the basis of the theory of shallow water waves. One can find, following this theory [6] and neglecting the difference between Lagrangian and Eulerian coordinates for small values that:

$$\sigma = -\rho g(h-y+\eta) - \rho g h_0^2 (h+\eta)_{xx}/3 + 4\mu^* u_x/3 + 4\eta^* u_{xt}/3. \qquad (1.2)$$

where h_0 is an averaged thickness of the layer and $(h\text{-}h_0)/h_0 << 1$, μ^* is an elastic shear modulus, η^* is a viscosity coefficient. A subscript 0 defines here and further undisturbed values. Below we will not take into account the fourth order, with respect to u, terms in (1.1) and (1.2). Moreover, nonlinear terms will be only considered which do not explicitly depend on the viscosity and dispersive coefficients. We assume that $g = g_0 + g_y$, where g_0 is the acceleration due to gravity, and g_y is the seismic-induced acceleration. It is also assumed that topographic terms similar to $\rho g h_x u_x$ and less are negligible. This simplifies the analysis of the influence of the nonlinearity, resonance and topography on the surface waves. Taking into account the comments above one can obtain from (1.1) and (1.2) that:

$$u_{tt} - a_0^2 u_{xx} = \beta u_x u_{xx} + \beta_1 u_{xx} u_x^2 + \mu u_{txx} + k u_{ttxx} - g h_x - g h_0^2 h_{xxx}/3, \qquad (1.3)$$

where $a_0^2 = a_h^2 + 4\mu^* \rho^{-1}/3$, $a_h^2 = gh$, $\beta = -3gh$, $\beta_1 = 6gh$, $\mu = 4\eta^* \rho^{-1}/3$ and $k = g h_0^3 a_0^{-2}/3$. The speed, a_0, of the shallow ground waves depends on the thickness of the layer and on the shear-wave speed. a_0 also depends on a perturbation g_y of g but we will neglect this dependence. If $\mu^* = 0$ equation (1.3) is valid for water waves. The nonlinear terms in (1.3) are of the second and third order. Generally speaking, the dissipative term is of first order but we will assume that this term and $k u_{ttxx}$ are of second order. The last terms in (1.3) take into account the topographic effects. The perturbation method allow to obtain the approximate solution of (1.3) [7]:

$$\begin{aligned}
u &= J_1(r) + j_1(s) + J_2(r) + j_2(s) + J_3(r) + j_3(s) \\
&-0.25 a^{-1} \iint g[h_s - h_r + h_0^2 a^{-2}(h_{ss} - 3h_{sr} + 3h_{rs} - h_{rr})/3] dr ds \\
&+A(r-s)\{[J_1'(r)]^2 + [j_1'(s)]^2\}/2 + \mu a_0^{-2}(s-r)[J_1''(r) - j_1''(s)]/4 \\
&+k a_0^{-2}(s-r)[J_1'''(r) - j_1'''(s)]/4 + A(r-s)[J_1'(r)J_2'(r) + j_1'(s)j_2'(s)] \qquad (1.4) \\
&+a\{j_1(s)[J_1'(r)]^2 + J_1(r)[j_1'(s)]^2\}/2 + (b - A^2/2)\left\{J_1'(r)\int [j_1'(s)]^2 ds + j_1'(s)\int [J_1'(r)]^2 dr\right\} \\
&+(c - 3A^2/2)(r-s)\{[j_1'(s)]^3 - [J_1'(r)]^3\} + A^2(r^2 - 2rs + s^2)\{J_1''(r)[J_1'(r)]^2 + j_1''(s)[j_1'(s)]^2\}.
\end{aligned}$$

Here $J_1(r), j_1(s), J_2(r), j_2(s), J_3(r), j_3(s)$ are unknown functions defined by boundary conditions, $A = \beta a_0^{-3}/4, a = 5A^2 - 2D, b = -2A^2 + D, c = -4a^2 + D, D = \beta_1/4a_0^4$ and $r = t - x a_0^{-1} + \beta u a_0^{-3}/4$ and $s = t + x a_0^{-1} - \beta u a_0^{-3}/4$. Expression (1.4) is only valid for periodical processes.

1.2. *Vertical waves*

If the thickness of the topographies increases then vertical waves are excited additionally to the surface waves. Let us consider these waves assuming that the thickness is much lesser then other dimensions of the hill (basin). So that to simplify the problem we will consider the vertical waves as independent from the surface waves and neglect by a variation of the

thickness of the hill (basin). Therefore the vertical waves may be considered as one-dimensional waves which propagate in the layer with parallel flat surfaces. Material of the layer will be simulate as a granular viscoelasic (the Kelvin model) medium saturated by the air-liquid mixture.

After the above assumptions our problem is reduced to a solution the next equations which are written for average values:

$$\rho_0 u_{tt} = \sigma_x \ , \tag{1.5}$$

$$\rho(1+u_x) = \rho_0 \ , \tag{1.6}$$

$$\sigma = -P + 4\mu^*(1+nV_0 - nV)u_x/3 + 4\eta^* u_{xt}/3 \ , \tag{1.7}$$

$$\rho = \rho_0[(1-n\,V_0)(1-P/K_B - \alpha p/K_B) + nV]^{-1}, \tag{1.8}$$

$$p_t - BP_t = k_1\eta_*^{-1}\eta_1(1-\alpha B)p_{xx} \ , \tag{1.9}$$

$$(p+Y)(p_0+Y)^{-1} = (\rho_l/\rho_{0l})^z, \tag{1.10}$$

where (1.5)-(1.9) are the motion, continuity, constitutive, state and hydraulic diffusivity [8] equations, respectively. Equation (1.10) is a state equation for bubbly liquid saturating of pores. In (1.5)-(1.9) x is a vertical and upwards Lagrangian coordinate; P is a pressure in the solid phase, respectively. Writing equation (1.7) we considered the granular material as the initially damaged material and took into account an influence of a variation of the damages (pores) on this equation [9]. We assumed that nV is of the porous volume per unit volume of the material. The state equation (1.8), where p is a pressure of the porous liquid and K_B is the bulk modulus of the equivalent dry material [8] is an analog of the state equation for bubbly liquid [10]. Following [8] we wrote the hydraulic diffusion equation (1.9) introducing the 'Skempton's coefficient' B, permeability coefficient k_1, Biot's modulus η_1, Biot's coefficient α, and viscosity coefficient η_* of bubbly liquid. We will study only compression-tension processes in plane waves therefore a liquid motion is connected with a change of the material volume. As a result there is the practically undrained deformation of the layer material in the above waves. Equation (1.10) was written following [11]. Value ρ_l is the average density of bubbly liquid and

$$Y = \frac{K_f(1-V_{0g}) + V_{0g}/(\gamma p_0)}{(\lambda+1)(1-V_{0g})K_f^2 + V_{0g}(\gamma+1)\gamma^{-2}p_0^{-2} - [K_f(1-V_{0g}) + V_{0g}/(\gamma p_0)]^2} - p_0 \ ,$$

$$z = \{[\,K_f(1-V_{0g}) + V_{0g}/(\gamma p_0)](p_0+Y)\}^{-1} \ , \qquad K_f = [\lambda(p_0+B_*)]^{-1} \ ,$$

where V_{0g}, λ and γ are the undisturbed volume of gas bubbles per unit volume of the liquid and the polytropic exponents of the fluid and air, respectively. Value B_* is a constant. For room temperature $\lambda = 7.15$ and $B_* = 304.5$ MPa. In the case of adiabatic oscillations of bubbles $\gamma = 1.4$, and $\gamma = 1$ in the case of isothermal ones. Assuming in (1.10) the gas volume $V_{0g} = 0$ or 1 we can obtain the state equation for fluid or gas, respectively. Since mass of the bubbly liquid in pores does not vary, a variation of the density of this liquid is defined by a variation of volume of the pores. Therefore we can rewrite equation (1.10) as

$$(p+Y)(p_0+Y)^{-1} = (V_0/V)^z. \tag{1.11}$$

It is emphasises that equations (1.5)-(1.9) and (1.11) describe waves in bubbly liquid if $\mu^* = 0$, $k_1 = 0$ and $\alpha = 0$. Equations (1.5)-(1.9) and (1.11) can be reduced to

$$u_{tt} - a_0^2 u_{xx} = \beta u_x u_{xx} + \beta_1 u_{xx} u_x^2 + \mu u_{xxt}, \tag{1.12}$$

where $a_0^2 = (4\mu^*/3 - b_1 B^{-1})\rho_0^{-1}$, $\beta = -4\mu^*\rho_0^{-1}[1 + b_1 K_M^{-1} + 1.5 b_2 B^{-1}/\mu^*]/3$,

$\beta_1 = -\rho_0^{-1}[4\mu^* b_2 K_M^{-1}/3 + 3b_3 B^{-1}]$, $\mu = [4\eta^*/3 + k b_1 \eta_*^{-1}\eta_1(B^{-1} - \alpha)a_0^{-2}]\rho_0^{-1}$ and

$K_M^{-1} = (1-V_0)(B^{-1}+\alpha)K_B^{-1}$, $b_1 = -z(p_0+Y)V_0^{-1}[1+z(p_0+Y)V_0^{-1}K_M^{-1}]^{-1}$,

$b_2 = -0.5(z+1)b_1V_0^{-1}[1+b_1K_M^{-1}]^2$, $b_3 = 0.5(z+1)b_1V_0^{-2}[a_1(z+1)K_M^{-1}+(z+2)/3][1+b_1K_M^{-1}]^3$.

Constitutive equation (1.7) may be written so that:

$$\sigma = -(b_1u_x+b_2u_x^2+b_3u_x^3)/B + k\eta_1\eta^{-1}(B^{-1}-\alpha)\int(b_1u_x+b_2u_x^2+b_3u_x^3)_{xx}dt + 4\mu^*[1-u_x$$

$$-K_M^{-1}(b_1u_x+b_2u_x^2)]u_x/3+4\eta^*u_{xt}/3 \quad . \qquad (1.13)$$

Equation (1.13) is valid for the weakly nonlinear granular media. But inside of the Tarzana hill the accelerations were close to 2 g_0 and strong nonlinear waves should be expected. Particularly, granular media (soil) demonstrate the different behaviour in tension and compression waves. In the tension waves the soil properties remind properties of bubbly liquid or gas. If an excited acceleration is greater than g_0, the resonator can periodically lose a contact with the bed. As a result the seismic waves are trapped by the resonator.

A strongly nonlinear constitutive equation was written for the dry undrained inviscid material:

$$\sigma = \tfrac{1}{2}K_MB^{-1}\{b-[b^2+4P_0V_0K_M^{-1}]^{0.5}\}+4\mu^*u_x/3\,, \qquad (1.14)$$

where $b = u_x+V_0-P_0K_M^{-1}$. According to (1.14) properties of the granular-type material inside of the tension waves is close to properties of gas. Equation (1.14) is an analog of the strongly nonlinear state equation discussed in [12] for water.

If $h_x = k = 0$ then equation (1.3) reduces to (1.12) and solution (1.4) is the solution of equation (1.12). Solution (1.4) is approximately valid both for elongated hills and valleys (basins) because we are modelling them as the infinite layer. However, we will mostly discuss the ground motion at the Tarzana hill. It is important for our model that the *P*-wave velocity a_0 'inside' of the Tarzana hill is approximately 520 m/s [2] while the *P*-wave velocity is 1100 m/s just 5 m below the base of the hill. Thus, near this base there is the *P*- wave velocity discontinuity. The seismic waves reflect practically completely from this discontinuity and as a result they are trapped by the hill.

2. Simulation of resonators with free boundary (hills and basins)

First, the horizontal waves in the hill is considered. The length of the hill is $2L$. The undisturbed hill surface is defined by the equality $y=h(x)$. The bottom of the hill is at $y=0$. Let a hill geometry be symmetrical with respect to the vertical $x = 0$, and $y=h(0)$ is the highest point of the hill top. A slope of the hill top with respect to the bottom of the hill is constant and very small ($h_x = \alpha << 1$). Lateral surfaces of the hill are perpendicular to the hill bottom and located at $x = \pm L$. Let the seismic-induced vertical acceleration be approximated by the periodical law: $g_y = \delta\cos\omega t$. At the lateral surfaces of the hill we have $\sigma = 0$. The hill is symmetrical therefore $u = 0$ $(x = 0)$, $\sigma = 0$ $(x = L)$. Finally the boundary conditions may be presented so that:

$$u = 0 \ (x = 0) \ , \ u_x = 0 \ (x = L). \qquad (2.1)$$

Let us consider the basin (valley). It is assumed that a basin free surface is flat, but the central point of the basin bottom is a lowest point of this surface. The point $x=0$ we locate at the left flank of the basin. The flanks are fixed. As a result the displacement $u=0$ at $x=0$ and at $x=2L$. Since the problem is completely symmetrical with respect to $x=L$ we have there $u_x = 0$. So the last problem is identical to the problem formulated above for the hill.

Considering the vertical waves we assume that the ground surface is free and the underlying surface of the layer is excited harmonically:

$$u_t = -\omega l\sin\omega t \ (x = 0) \ , \ u_x = 0 \ (x = L). \qquad (2.2)$$

One can see that the formulated above problems for the vertical and horizontal waves are the same since h_x is constant and $g_y = \delta\cos\omega t$ for the horizontal waves. An expression defining the resonant frequencies follows from the linear solution of the problem:

$\Omega_N = (N - 1/2)\pi a_0 / L$ (N=1, 2, 3, ..). (2.3)

Together with (2.3), according to the nonlinear correction of the linear solution, there are the so-called quadratic resonant frequencies:

$\Omega_N^* = (N - 1/2)\pi a_0 / 2L$. (2.4)

We must emphases that expressions (2.3) and (2.4) are valid both for horizontal and vertical waves but a_0 and L are fifferent vary for those cases.

Let us calculate the first two resonant frequencies of the hill using formula (2.3) which takes into account both the height and length of the Tarzana hill. Following [2] we will take the largest (L =250 m) and smallest (L=100 m) dimensions of the hill and assume that the shear-wave speed equal to 249 m/s. Then for L =250 m we have Ω_1 = 1.77 and Ω_2 =5.3 Hz. These values correlate well with frequency peaks presented in Fig. 6 from [2]. For L =100 m we have Ω_1 = 4.42 and Ω_2 =13.2 Hz. The frequency Ω_1 = 4.42 Hz correlates with main frequency peak (3.26 Hz) presented in Fig. 6 from [2]. It is easy to find from (2.3) the dimension (L =139 m) of the hill which corresponds to the above main frequency peak. For this dimension (the dimension depends on the direction of measuring the hill) we have Ω_1 = 3.26 and Ω_2 = 9.78 Hz. The last value correlates with the second main frequency peak (8.6-8.8 Hz). Rail [2] identifies this peak as a possible first vertical overtone. However, the average P-wave velocity between the base and the top of the hill was 578±60 m/s, therefore we explain the above second main frequency peak by the second resonance of the horizontal oscillations. So the formula (2.3) describes some results of the calculations and observations.

Let us construct solutions which are valid near and at resonances (2.3) and (2.4). For the resonant frequencies (2.3) and μ =0 the boundary conditions give the next basic equation:

$-\omega^* F' - k a_0^{-3} L F''' + a_0^{-3} L (F')^3 / 8 = l \cos\omega t$. (2.5)

Here $F' = J_1'(t + L/a_0)$ and $\omega^* F'$ takes into account contributions from the off-resonance effects. First we consider the nonlinear effect. If $\omega^* = k$=0 we have

$F'(t \pm (x - L)/a_0) = 2a_0[lL^{-1} \cos\omega(t \pm x/a_0)]^{1/3}$. (2.6)

Now the elevation and horizontal acceleration may be calculated

$\eta = h[F'(r + L/a_0) - F'(s - L/a_0)]/a_0$, $u_n = F''(r + L/a_0) + F''(s - L/a_0)$ (2.7)

The expression for F' (which is valid if the influence of the dispersion on equation (2.5) is small and localises at and near $\omega t = n\pi - \arccos|R|$, where $R = -2^{5/3} a_0 \omega^* (Ll^2)^{-1/3} / 3)$ is

$F' = 4a_0(\omega^* \omega^{-1})^{0.5} \Phi(t + La_0^{-1})[1 - |\Phi(t + La_0^{-1})|] + 2a_0(lL^{-1})^{1/3} y$. (2.8)

Here $\Phi(t + La_0^{-1}) = \tanh[-a_0 \omega^{-1} (\omega^* \omega^{-1} k^{-1})^{0.5} \cos(\omega t + \arccos|R|)]$ and it is assumed that $a_0 \omega^{-1} (\omega^* \omega^{-1} k^{-1})^{0.5} >> 1$. If $R > 0$ we have in (2.8) that

$y = -2R_1 \sinh[\frac{1}{3} a \sinh(0.5 R_1^{-3} \cos\omega t)]$, (2.9)

where $R_1 = 2^{-1/3} (sign \cos\omega t) |R|^{0.5}$. Expression (2.9) is valid behind the resonant frequency where $\omega^* < 0$. If $-1 \le R < 0$ ($\omega^* > 0$) there is no continuous single-valued solution for y, and it is necessary to accept solution with discontinuties:

$y = -2R_1 \cosh[\frac{1}{3} \arccos h(0.5 R_1^{-3} \cos\omega t)]$; $-2R_1 \cos[\frac{1}{3} \arccos(0.5 R_1^{-3} \cos\omega t)]$;

$-2R_1 \cos[\frac{1}{3} \arccos(0.5 R_1^{-3} \cos\omega t) + 2\pi/3]$; $-2R_1 \cosh[\frac{1}{3} \arccos h(0.5 R_1^{-3} \cos\omega t)]$;

$-2R_1 \cos[\frac{1}{3} \arccos(0.5 R_1^{-3} \cos\omega t)]$; $-2R_1 \cos[\frac{1}{3} \arccos(0.5 R_1^{-3} \cos\omega t) + 2\pi/3]$;

$-2R_1 \cosh[\frac{1}{3} \arccos h(0.5 R_1^{-3} \cos\omega t)]$, (2.10)

which is valid for $0 < \omega t \le \arccos|R|$; $\arccos|R| < \omega t \le \pi/2$; $\pi/2 < \omega t < \pi - \arccos|R|$;

$\pi - \arccos|R| < \omega t \le \pi + \arccos|R|$; $\pi + \arccos|R| < \omega t \le 2\pi / 3$; $3\pi / 2 < \omega t < 2\pi - \arccos|R|$; $2\pi - \arccos|R| < \omega t \le 2\pi$, respectively.

If $R < -1$ there are three continuous expressions for y:

$$y = -2R_1 \cos[\tfrac{1}{3} a \cos(0.5R_1^{-3} \cos\omega t) + 2(i-1)\pi / 3], \qquad i = 1;2;3. \tag{2.11}$$

It is to be emphasised that there is also the acoustic solution. Generally speaking, the first term in (2.8), which takes into account dispersion, may be very small. Solution (2.8) describes shock-like waves generated if $-1<R<0$. Thus, solution (2.8) is not symmetrical respectively resonant frequency.

Generally speaking, acoustics and nonlinear (2.8) solutions may be used for description of different scenarios an off-resonant evolution of waves. Particularly they take into account hysteresis in earth material under dynamic resonance discussed in [13]. In Figures 1 and 2 an evolution of the resonant elevation wave is presented when the excited frequency increases and decreases through a resonance, respectively. The amplitude $l = 10^{-8}$ m. The curves (*****) were calculated according to the acoustic solution. The other curves were calculated according to (2.8). The intensive shock-like waves are generated if the excited frequency decreases (see Fig. 2).

Now using (2.7) we can write expressions for the resonant travelling waves. For example, for the travelling waves of the acceleration we have

$$F''[t \pm (x-L)/a_0] = 4a_0^2 \omega^* \omega^{-1} k^{-0.5} \sin\omega p_* \sec h^2[-a_0 \omega^{-1} (\omega^* \omega^{-1} k^{-1})^{0.5} \cos\omega p_*]$$
$$+2a_0 (lL^{-1})^{1/3} y_t(t \pm x/a_0) \quad , \tag{2.12}$$

where $p_* = t \pm x/a_0 + \omega^{-1} \arccos|R|$. The first term in (2.12) takes into account the dispersive effect which accumulates near lines where $\omega p_* = \pi n$. One can see that the dispersive effect is very important for acceleration waves. Particularly, the first term in (2.12) may be larger than the second term. Expressions (2.8) and (2.12) are valid if $R < 0$ ($\omega^* > 0$). For case $R > 0$ ($\omega^* < 0$) the first terms in (2.8) and (2.12) are absent.

From (2.12) it is follows that during the half period of the excitation the travelling waves recall solitons (peaks) and at the next half of the excitation the travelling waves recall antisolitons (crates) exist. These oscillating excitations recall so-called, recently experimentally discovered, *oscillons* [3]. By contrast with oscillons solution (2.12) describes *travelling oscillons.*

In Fig. 3 the travelling oscillon is presented. We assumed that $R = 0.3$, $l = 10^{-8}$ m and $L = 139$ m, $h = 20$ m. The dimensionless time ωt is used. The length is $1-x/L$ and $N = 1$. The right-hand side half of the hill is considered. One can see in Fig. 3 the oscillon travelling up to the hilltop and down to the lateral surface of the hill. We recall that the wave, which is symmetrical presented in Fig. 3, exists on the left-hand side of the hill. An maximum amplitude of the wave is approximately equal to the peak of the acceleration at the Tarzana hill. This maximum is on the flank of our pattern, where peaks follow after craters and vise versa. This maximum reduces and the oscillation profile varies when the distance from the lateral surface increases. At approximately $x=L/2$ the oscillations reminiscent of a shock wave having two peaks are generated. An increase the distance leads to steepening of those waves. Thus, according to the theory, the largest resonant amplification of the acceleration takes place near the edges of the pattern. However, this amplification may be very local and it affects only high harmonics. Near the centre of the hill the amplification may be smaller but affects both high and low frequency harmonics. In Fig. 4 the curves are presented which were calculated for $R = -0.3$ at $x = 0.9\,L$ (____) and $x = L/2$ (- - - -). For us it is important that the some curves in Figures 3 and 4 are practically the same as the shock-like and oscillon-like oscillations excited during of earthquake modelling (see Figures 14, 16, 18 and 21 from [14]).

Quantity of the oscillons, travelling up and down along of the hill, depend on the excited

frequency and equal $2N$. They can form different patterns. One of them, calculated for R = 0.0.5, $l = 10^{-8}$ m and N =4, displays in Fig. 5. One can see that along of the hill the standing oscillons are organised as a result of collisions of the travelling oscillons. A generation of these oscillons reminds the generation of the standing waves in linear acoustics but here we have nonlinear effect and the standing oscillons may be very strongly localised on the surface of the hill.

Let us consider earthquake-induced waves near the quadratic resonant frequencies (2.4). The boundary conditions give the next basic equation if the dissipative effect is negligible:

$$F_{-1}^{'} + F_{+1}^{'} - 2A(F_{-1}F_{-1}^{''} - F_{+1}F_{+1}^{''}) = -\omega l \sin\omega t \quad . \qquad (2.13)$$

Subharmonic oscillations are generated in a granular media under vertical vibrations if the acceleration amplitude larger than g_0 [3,4]. Since the peak acceleration of $1.82\, g_0$ was recorded at Tarzana hill we will try to consider strongly nonlinear effect, namely, the subharmonic oscillations of the topographies. Of course, our theories are not valid for strongly nonlinear oscillations, therefore we hope to obtain very rough qualitative result. For the left- and right- travelling waves we write approximately that

$$F_{\pm 1}^{'} = F'(t \pm xa_0^{-1}) = A_1 \sin\omega[t \pm (x - L)a_0^{-1}] + A_2 \sin\tfrac{1}{2}\omega[t \pm (x - L)a_0^{-1}], \qquad (2.14)$$

where $A_1 = 0.4A^{-1}\cot(0.5\omega La_0^{-1})$,

$A_2 = \{0.1A^{-2}[5A\omega l + 4\cot(0.5\omega La_0^{-1})\cos(\omega La_0^{-1})]/\sin(\omega La_0^{-1})\}^{0.5}$.

Now using (2.14) and (1.14) one can calculate the strongly nonlinear P - waves. A profile of the waves ($-\sigma$) for the Tarzana hill are presented in Fig. 6. The dotted line is motion of the hill bottom. The amplitude of the waves weakly depends on l and V_0 .We used for calculations parameters of sand and l =0.002 m , V_0 =0.5. Those waves are an analog the strongly nonlinear water waves excited in the vertical tube by the piston [15, 16]. Sometimes the subharmonic oscillations were excited in the tube if the water lost contact with the piston.

Let us consider the vertical motion of ground at the Tarzana hill using the presented above results. Observations (see Fig. 3 from [2]) showed resonant-like peaks of the P-wave amplitudes near frequencies 9 and 21 Hz. The second peak (21 Hz) is the first quadratic resonant peak of the hill since $h \approx 20$ m . We assume that the frequency of the vertical excitation of the hill was approximately 21 Hz. Then, according to solution (2.14), this excitation generated in the hill oscillations with frequency 10.5 Hz. So the first peak in Fig. 3 from [2] is a result of the excitation of subharmonical vertical oscillations of the Tarzana hill.

We have considered the natural resonators with free boundary. Trains of the tsunami-like surface waves and the compression shock-like waves may be excited there by earthquakes. These waves may become trapped because of reverberations. Because of reverberations and the slope (or curvature) of the boundaries the waves can change their frequency [1]. If this frequency increases then their amplitude reduces (see Fig. 1). However if the frequency of the trapped waves reduces then their amplitude strongly increases (see Fig. 2). Therefore a collapse of structure on the surface of the natural resonators can occur when the initial seismic waves had passed if the frequency of the reverberations of the trapped waves inside of the resonator reduces.

3. Solutions for resonators with fixed boundary

Here we consider examples of the resonators with the fixed boundary. Models of porous media are used. However results, which will be presented, are valid for all considered above media.

3.1.*Micromechanical analysis*

A simplified model of the porous element with a single pore is considered. We will consider below a case of oscillations of the pore containing the bubbly liquid. Motion of the material surrounding of the pore is described by the continuity and motion equations:

$\rho_t + v\rho_r + \rho v_r + 2\rho v/r = 0$, (3.1)

$\rho(w_{tt} + w_t w_{tr}) = \sigma^*_{r,r} + 2(\sigma^*_r - \sigma^*_\varphi)/r$, (3.2)

where $\sigma_r = -\alpha p + \sigma^*_r = -\alpha p + \lambda_*(w_r + 2w/r) + 2\mu^* w_r + 4\eta^*(w_{tr} - w_t/r)/3$,

$\sigma_\varphi = -\alpha p + \sigma^*_\varphi = -\alpha p + \lambda_*(w_r + 2w/r) + 2\mu^* w/r - 2\eta^*(w_{tr} - w_t/r)/3$, σ_r and σ_φ are the radial and transverse effective stresses, respectively. We will assume below that $\alpha = nV$, where V is of the volume of pores, n is the porous quantity per unit volume of the material. At a surface of the pore $r=R$ kinematic and force conditions are written: $w_t = R_t$, $\sigma^*_r = -p$. Generally speaking, the porous material is a compressible medium but we will assume that one to be incompressible considering the single pore: $\rho = \rho_0$. Integrating equations (3.2) we obtain

$$\rho_0(RR_{tt} + 3R_t^2/2) = \sigma^*_{r\infty} - p - 4\mu^*(1 - R_0^3 R^{-3})/3 + 4\eta^* R^{-1} R_t \quad , \qquad (3.3)$$

where $\sigma^*_{r\infty}$ is the total radial stress into infinity. The equation (3.3) is valid for the oscillations of voids and saturated pores in the elastic media. An influence of the inclusion takes into account the term p in equation (3.3). If $p=0$ we have the case of the void. Equation (3.3) contains three unknowns: R , $\sigma^*_{r\infty}$ and p, and connects the microvalue R with the macrovalues $\sigma^*_{r\infty}$ and p. Now we re-write equation (3.3) with help (1.11):

$$\rho_0(RR_{tt} + 3R_t^2/2) = \sigma^*_{r\infty} - [(p_0 + Y)(R_0/R)^{3z} - Y] - 4\mu^*(1 - R_0^3 R^{-3})/3 + 4\eta^* R^{-1} R_t \ . \qquad (3.4)$$

Equation (3.4) connects the microvalue R with the macrovalue $\sigma^*_{r\infty}$.

3.2.*Macromechanical analysis*

We assume that $\sigma^*_{r\infty} = \sigma$. Then equations (1.5)-(1.9) and (3.4) may be reduced, after some assumptions, to the next equation:

$$u_{tt} - a_0^2 u_{xx} = \beta u_x u_{xx} + \beta_1 u_{xx} u_x^2 + \omega_p^{-2} A_1 (u_{tt} - a_1^2 u_{xx})_{tt} + \mu_1 (u_{tt} - a_2^2 u_{xx})_t + \mu_b u_{xxtt} , \qquad (3.5)$$

where the coefficients are very complex. We only present here coefficients for the dry material ($p=0$) and bubbly liquid. For the case of dry pores $\omega_p^2 = 4\mu^*/\rho_0 R_0^2$,

$A_1 = -\rho_0 B_k / (4n\pi\omega_p^{-2} R_0$

$+\rho_0 B_k)$, $a_0^2 = [K_B + 4\mu^*(1 - nV_0)/3]/[\rho_0(1 - nV_0) + 4\pi n K_B R_0 \omega_p^{-2}]$, $B_k = (1 - nV_0)/K_B$,

$\beta = -2\beta_* \omega_p^2 (4\pi n R_0 + \rho_0 \omega_p^2 B_k)^{-1}[4\mu^* B_k/3 + \beta_*/(nV_0)]$, $\beta_* = 1 + 4\mu^* B_k/3 - \rho_0 a_0^2 B_k$,

$\beta_1 = 8\beta(\mu^*)^2 B_k^2 (3nV_0 + 4\mu^* B_k)^{-1} + \beta_* \rho_0^{-1}(3nV_0 + 4\mu^* B_k)^{-1}[12\mu^* \beta \rho_0 B_k (nV_0)^{-1} + 64(\mu^*)^3 B_k^2/3$

$+32\beta_*(\mu^*)^2 B_k (nV_0)^{-1} + 12\mu^* \beta_*^2 (nV_0)^{-2}]$, $a_1^2 = (1 + 4\mu^* B_k/3)/(\rho_0 B_k) - 16(\eta^*)^2 \rho_0^{-2} R_0^2/3$

$\mu_1 = 4\eta^* B_k R_0^{-2}/(4n\pi R_0 + \rho_0 \omega_p^2 B_k)$, $a_2^2 = (1 + 4\mu^* B_k/3)/(\rho_0 B_k) - \omega_p^2 R_0^2/3$,

$\mu_b = 4\eta^* B_k/(12n\pi R_0 + 3\rho_0 \omega_p^2 B_k)$. For the bubbly liquid we have in (3.5) that

$a_0^2 = \rho_0^{-1}[(1 - nV_0)\rho_{0l}^{-1} a_l^{-2} + nV_0/(\gamma p_0)]^{-1}$, $\beta = -\rho_0^2 a_0^6 [(1 - nV_0)(1 + \lambda)\lambda^{-2}(p_0 + B_*)^{-2} + nV_0(1$

$+\gamma)\gamma^{-2} p_0^{-2}]$, $\omega_b^2 = 3\gamma p_0 \rho_{0l}^{-1} R_0^{-2}$, $A_1 = 1 + 16(\eta^*)^2 \omega_b^2 (1 - nV_0)(9\gamma p_0 \rho_{0l} a_l^2)^{-1}$, $a_l^2 = \lambda(p_0 + B_*)\rho_{0l}^{-1}$,

$a_1^{-2} = \rho_0(1 - nV_0)[\lambda A_1 (p_0 + B_*)]^{-1}$, $\mu_1 = 4\eta^* \rho_0^{-1}[1 + \rho_0 a_0^2 (\gamma p_0)^{-1}]/3$,

$a_2^{-2} = 4\eta^* \mu_1^{-1} \rho_0 a_0^2 (1 - nV_0)/[3\gamma\lambda p_0 (p_0 + B_*)]$, $\mu_b = 4\eta^* \lambda^{-1} a_0^2 \omega_b^{-2} (1 - nV_0)/(3p_0 + 3B_*)$ and

ρ_{0l} is a liquid density. A solution of equation (3.5) is (1.4) if interactions of the nonlinear, dispersive and dissipative effects are negligible. The solution (1.4) must satisfy the next boundary conditions:

$u = 0 \quad (x = 0)$, $\quad u = l\cos\omega t + d \quad (x = L)$, (3.6)

where l and d are constants whose values are of the same order. From the linear solution of the problem it follows an expression defining the resonant frequencies: $\Omega_N = N\pi a_0 / L$.
Together with these frequencies, according to the nonlinear correction of the linear solution, there are quadratic resonant frequencies which coincide with (2.3). Let us construct solutions which are valid near and at $\Omega_N = N\pi a_0 / L$. The boundary conditions (3.6) give the next basic equation [17]:

$$-2N\pi\omega^{*}\omega^{-2}F^{'} - \beta L a_0^{-4}(F^{'})^2/2 + \mu L a_0^{-3}F^{*} + k L a_0^{-3}F^{'''} = l\cos\omega t + d, \qquad (3.7)$$

Let us consider a case when the dispersive effect is greater than the dissipative effect. Then, for the right - and left- hand side travelling wave we have

$$u_p = 2R\sqrt{\varepsilon}\pi^{-1} + \sqrt{\varepsilon}\{3\mathrm{sech}^2[(\sin p - R)/\sqrt{2q_0}] - 1\}\cos p, \qquad (3.8)$$

where $p=\omega[t\pm(x-L+\beta a_0^{-2}u/4)/a_0]/2$, $q_0 = -ka_0\omega^2/(2\beta\sqrt{\varepsilon})$, $\varepsilon=-4la_0^4(\beta L)^{-1}$ and $R=-\pi\omega^{*}a_0^3(\beta\omega\sqrt{\varepsilon})^{-1}$ $(-1 \le R \le 1)$ [17]. Expression (3.8) is valid for the even resonances and defines subharmonic oscillations with frequency $\omega t/2$. A peak is generated during one cycle of the excitation,; on the next cycle a crater is generated. Thus this excitation is reminiscent of the travelling oscillon (2.12). In Fig. 7 the travelling oscillon trapped between points $x = 0$ and $x = L/2$, and the travelling oscillon trapped between points $x = L/2$ and $x = L$ are presented. When the cycle of the excitation changes, the travelling peaks transform to the travelling craters and vice versa at point $x = L/2$. One can see in Fig. 8 that along the resonator the standing oscillons are organised as a result of a collision of the two travelling oscillons. Calculations showed that 2 N travelling oscillons formed N standing oscillons.
For the general case we can write the next solution of (3.7):

$$F^{'}(t \pm x a_0^{-1}) = 2R\sqrt{\varepsilon}/\pi + \sqrt{\varepsilon}\tanh\{2\sqrt{q}(\sin p_{*} - R) - q_1\tanh^2[2\sqrt{q}(\sin p_{*} - R)]\}\cos p_{*} \times$$

$$\times \mathrm{H}(R - \sin p_{*}) + \sqrt{\varepsilon}\{\tanh[2\sqrt{q}(\sin p_{*} - R)] - |q_1|\tanh^2[2\sqrt{q}(\sin p_{*} - R)]$$

$$+(2|q_1| + q_0)\exp[-\mu_{*}(p_{*} - \Delta)]\sin^2[(p_{*} - \Delta)/\sqrt{2q_0}]\}\cos p_{*} H(\sin p_{*} - R), \qquad (3.9)$$

where H is the Heaviside function, $\sqrt{q} = -\beta\sqrt{\varepsilon}/(2\eta_{*}\omega a_0)$, $q_1 = k\beta\sqrt{\varepsilon}\mu_{*}^{-2}/(2a_0)$, $\mu_{*} = \eta_{*}(k\omega)^{-1}$ and $\Delta = \arcsin R$. Curve calculated according to (3.10) are presented in Figure 9 and 10. The curves corresponding to experimental curves in Figures 18 and 7 (r =-0.62;-0.3;0.23;0.64 and 1.22) from [18]. We used the parameters presented in [18]. A coefficient of a bottom friction $\mu = 40$ cm^2/sec and $\mu_{*} = 0$.
Let us write the basic equation for the quadratic resonances $\Omega_N = (N - 1/2)\pi a_0 / L$:

$$-(2N-1)\pi\omega^{*}\omega^{-2}F^{'} - \beta L a_0^{-4}(F^{'})^2/2 + \mu^{*} L a_0^{-3}F^{''} + k L a_0^{-3}F^{'''} = l_1\cos 2\omega t + d_1 \qquad (3.10)$$

where $F^{'} = J_2^{'}(t + L/a_0)$. Equation (3.10) differs from (3.8) only in some coefficients.
Therefore all the results obtained for equation (3.7) are valid for (3.11).
The presented above results may be interesting for all natural resonators (hills, valleys, likes and so on) for which equation similar to (1.3) (or (3.5)) and boundary conditions (2.1), (2.2) or (3.7) are valid.
Conclusion. Thus the theory of the natural resonators is presented. The waves in the resonators are described by the modified Boussinesq type equations. The theory takes into account the influence both the physical phenomena and the topography on the earthquake-induced waves. The theory predicts strong amplification of the seismic waves due to resonances. The resonant effect depends on the topography, boundaries of resonators and an intensity of earthquake.

References . **1**. Rail, J.A., Saltzman, N.G. & Ling, H. 1992 *Am. Sci.* Nov-Des, 566. **2**. Rail, J. A. 1996 *Bull. Seism. Soc. Am.* 86, 1714. **3**. Umbanhowar, P. B., Melo, F. & Swimmey, H. L. 1996 Nature 382 , 793. **4**. Jaeger, H. M., Nagel, S. R. & Behringer, R. P. 1996 Rev. Mod. Phys. 68, 1259. **5**. Lamb, H. 1932 *Hydrodynamics*. Cambridge University Press. **6**. Chester, W. 1968 *Proc. R. Soc. Lond. A* 377, 449. **7**. Galiev, Sh. U. 1972 *Izv. Akad. Nauk SSSR, Mech. Tverdogo Tela* 4 , 80. **8**. Charlez, P.A. 1991 *Rock Mechanics.* Volume 1. Editions Technip, Paris. **9**. Rabotnov Yu. N. 1969 *Creep Problems in Structural Members.* North- Holland, Amsterdam. **10**. Rudenko, O.V. & Soluyan, S. I. 1977 *Theoretical Foundations of Nonlinear Acoustics.* Consultants Bureau, Plenum. **11**. Galiev, Sh. U. & Panova, O. P. 1995 *Strength Math.* 27, 602. **12**. Galiev, Sh.U. 1997 *Int.J. Impact Engng* 19, 345. **13**. Kadish, A.& Johnson, P.A. 1996 *J. Geophys. Res.* 101, 25,139-25,147. **14**. Zeng, X. & Schofield, A.N. 1996 *Geotechnique* 46, 83. **15**. Galiev, Sh. U. 1988 *Nonlinear Waves in Bounded Continua.* Kiev, Naukova Dumka (in Russian). **16**. Natanzon, M.S. 1965 *Izv.Akad. Nauk SSSR Mekh.* 5, 14. **17**. Galiev, Sh.U. & Galiev, T.Sh.1997 , submitted to *Phys. Lett. A*. **18**. Chester, W. & Bones, J. A. 1968 *Proc. R. Soc. Lond. A* 306, 23.

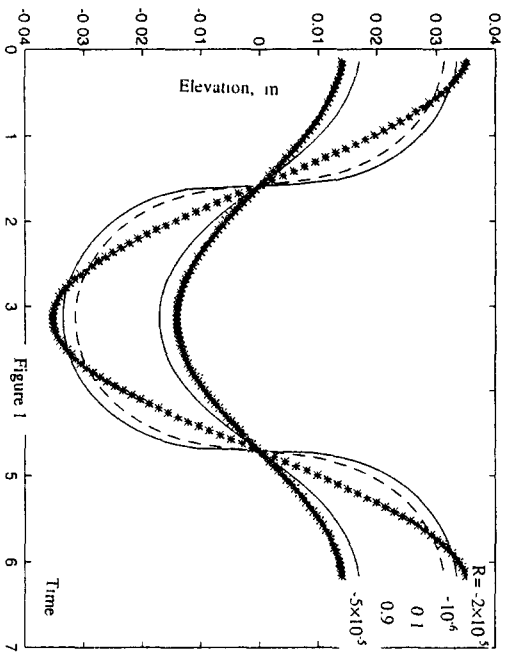

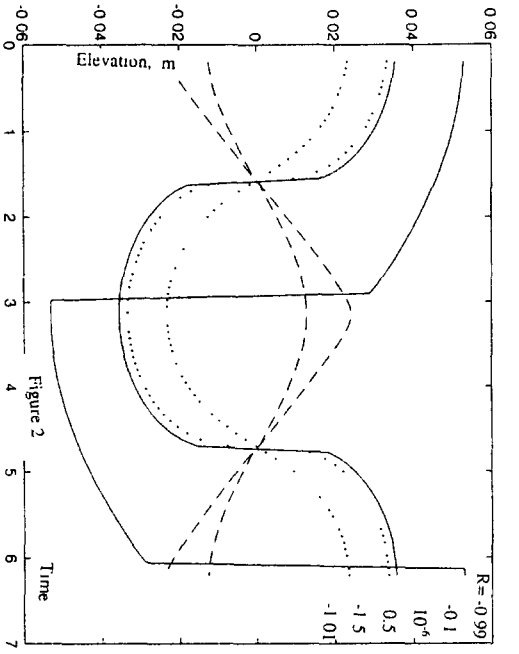

Figure 3

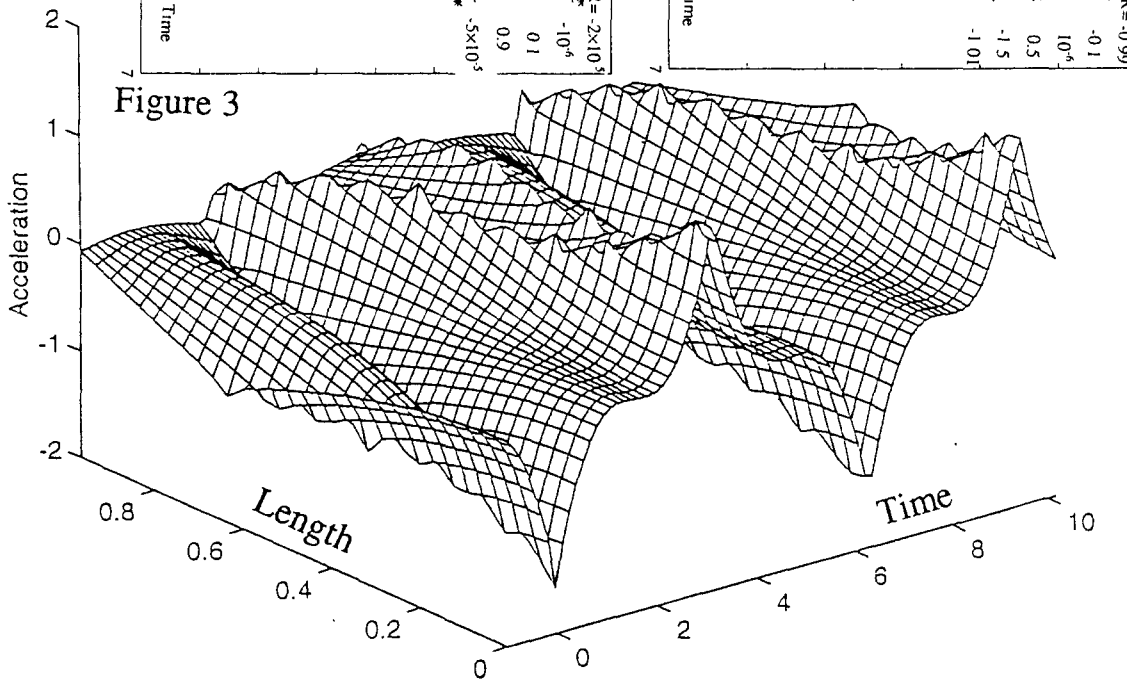

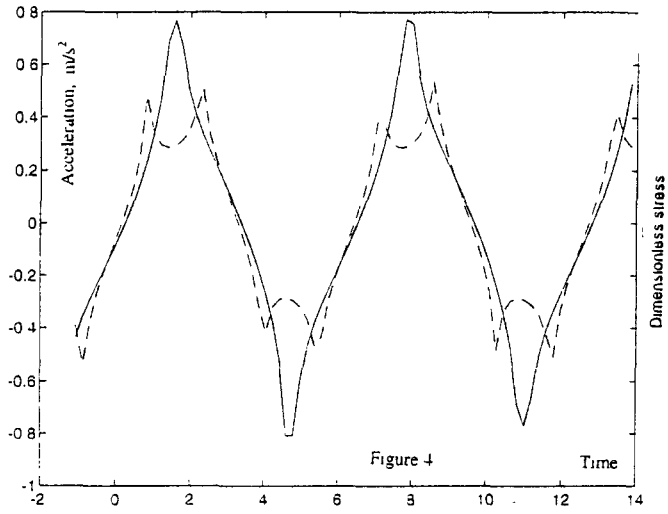

Figure 4

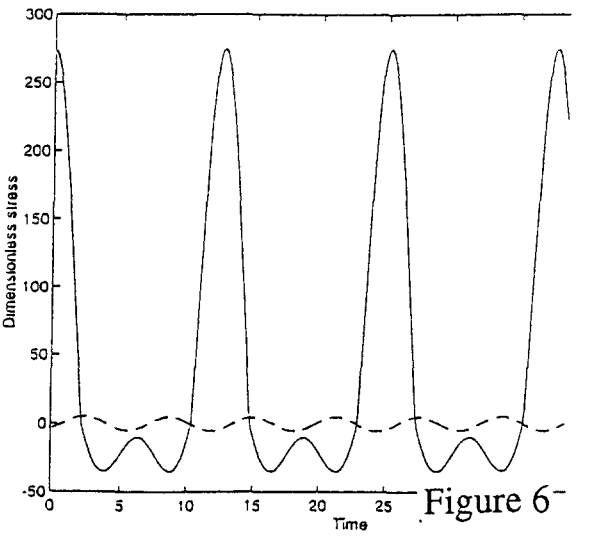

Figure 6

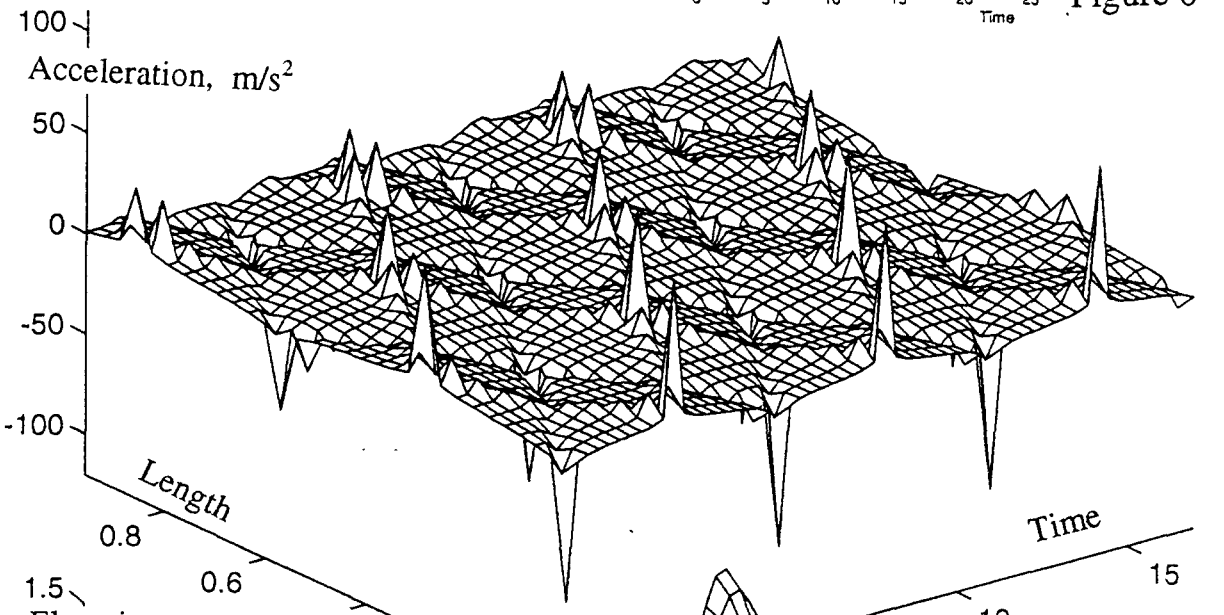

Figure 5

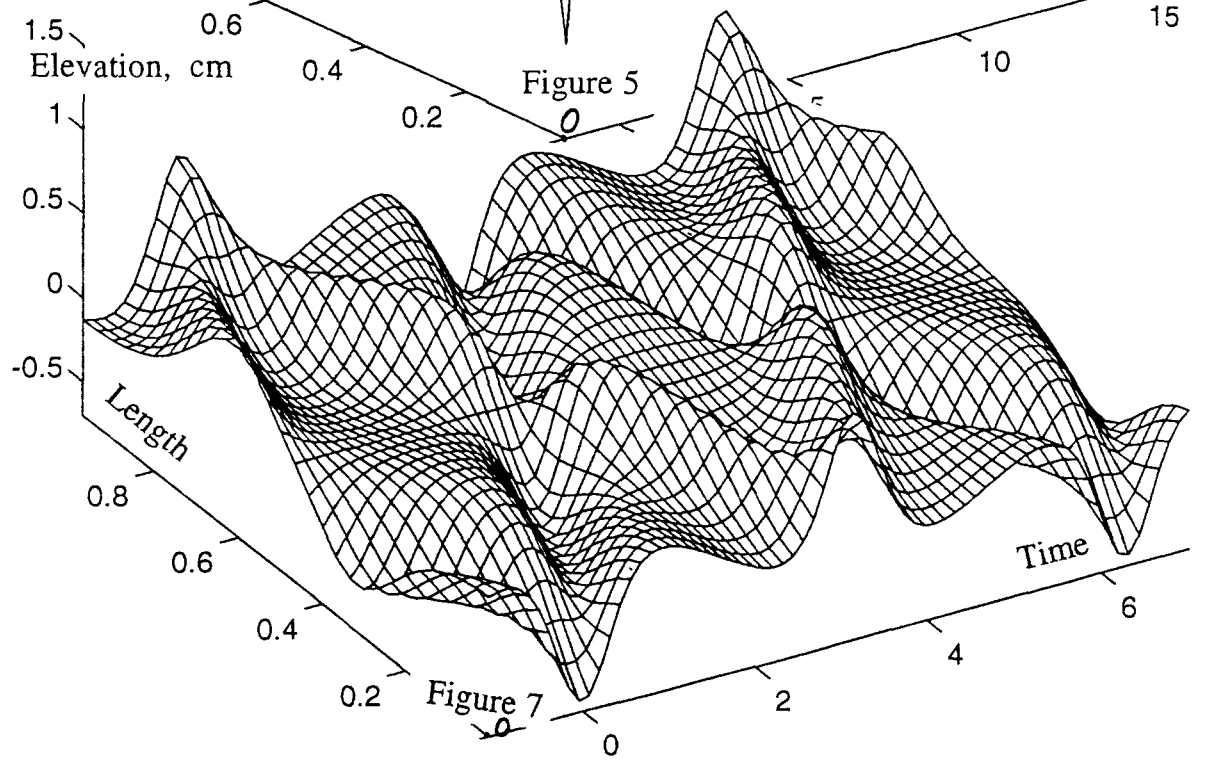

Figure 7

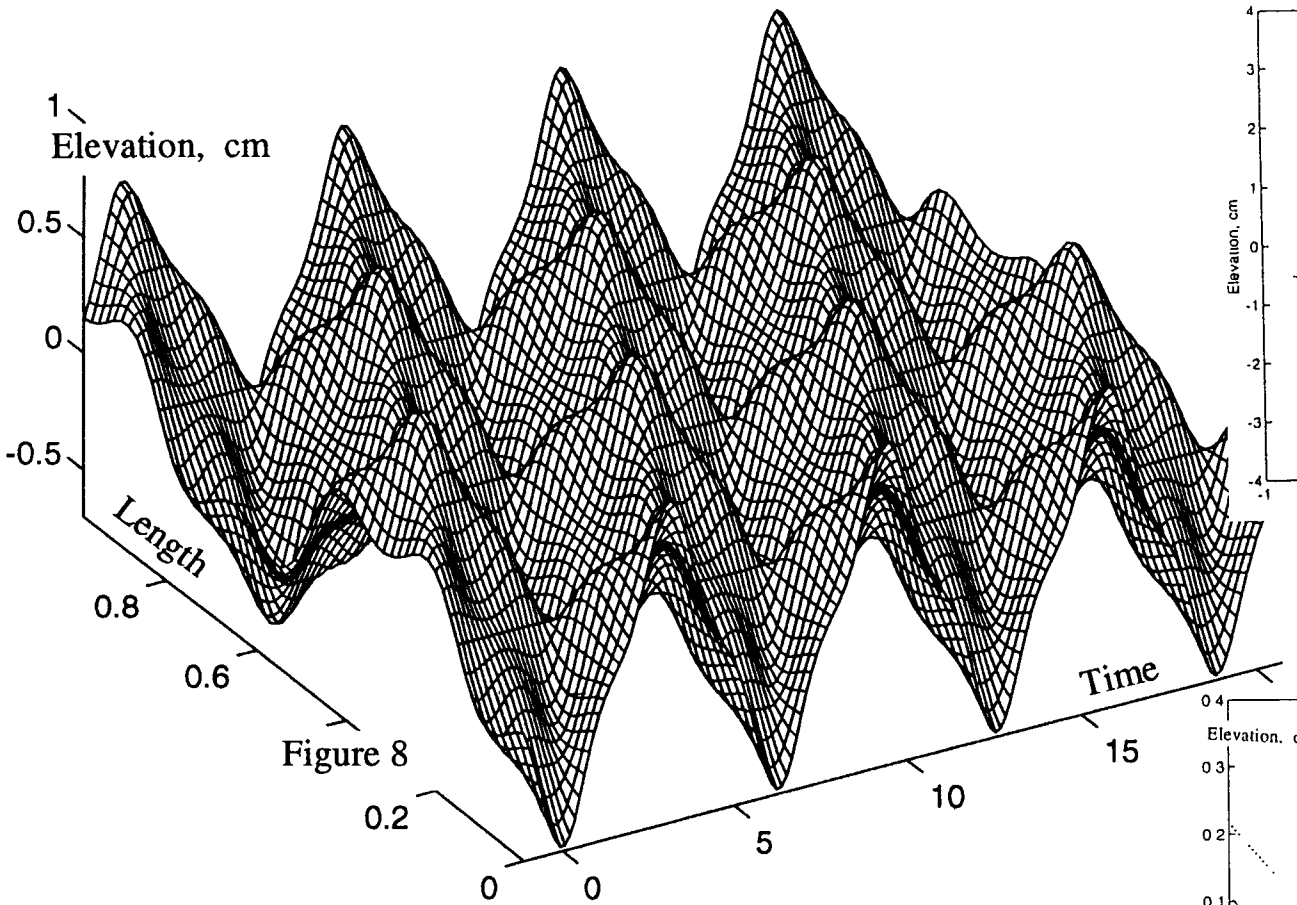

Figure 8

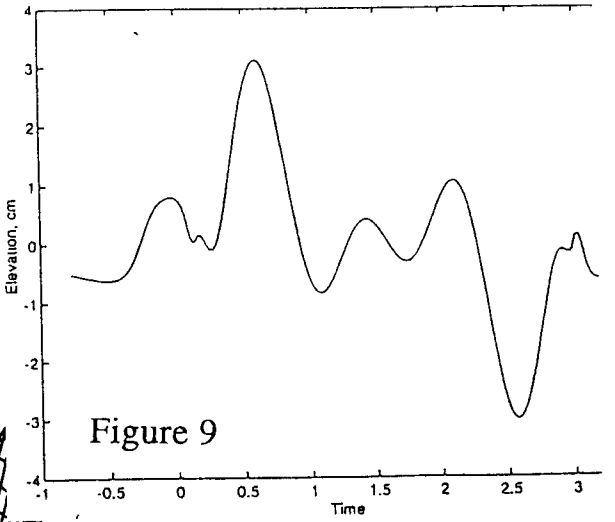

Figure 9

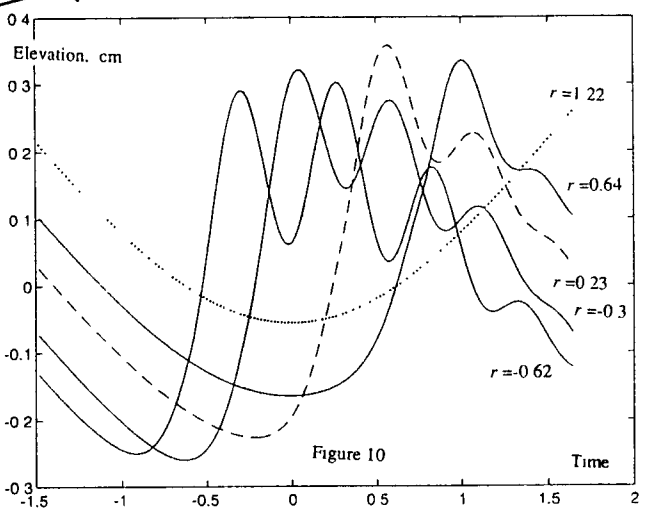

Figure 10